

---

# Contrastive Representation Distillation via Multi-Scale Feature Decoupling

---

Cuipeng Wang<sup>1</sup>, Tiejuan Chen<sup>2</sup>, Haipeng Wang<sup>1\*</sup>

<sup>1</sup> Key Laboratory for Information Science of Electromagnetic Waves,  
Ministry of Education Fudan University,  
University of Fudan, <sup>2</sup> Shanghai Jiao Tong University

23110720121@m.fudan.edu.cn, tieyuanchen@sjtu.edu.cn, hpwang@fudan.edu.cn

## Abstract

Knowledge distillation is a technique aimed at enhancing the performance of a small student network without increasing its parameter size by transferring knowledge from a large, pre-trained teacher network. In the feature space, different local regions within an individual global feature map often encode distinct yet interdependent semantic information. However, previous methods mainly focus on transferring global feature knowledge, neglecting the decoupling of interdependent local regions within an individual global feature, which often results in suboptimal performance. To address this limitation, we propose **MSDCRD**, a novel contrastive representation distillation approach that explicitly performs multi-scale decoupling within the feature space. MSDCRD employs a multi-scale sliding-window pooling approach within the feature space to capture representations at various granularities effectively. This, in conjunction with sample categorization, facilitates efficient multi-scale feature decoupling. When integrated with a novel and effective contrastive loss function, this forms the core of MSDCRD. Feature representations differ significantly across network architectures, and this divergence becomes more pronounced in heterogeneous models, making feature distillation in heterogeneous models notably more challenging. Despite this, our method not only achieves superior performance in homogeneous models but also enables efficient feature knowledge transfer across a variety of heterogeneous teacher-student pairs, highlighting its strong generalizability. Moreover, its plug-and-play and parameter-free nature enables flexible integration with different visual tasks. Extensive experiments on different visual benchmarks consistently confirm the superiority of our method in enhancing the performance of student models.

## 1 Introduction

The past few decades have witnessed remarkable achievements of neural networks in the field of computer vision. With the continuous increase in network depth and width [1], model performance has also been significantly improved. Deeper networks with more parameters have brought improved performance; however, they also come with trade-offs. Deeper networks incur higher computational and memory overhead, posing significant challenges for deployment on resource-limited devices. To address this issue, various model compression techniques have been proposed, including model pruning [2, 3, 4, 5], model quantization [6, 7], lightweight network design [8, 9, 10], and knowledge distillation [11, 12, 13].

Knowledge distillation is a specialized form of transfer learning, where the “knowledge” from a large pre-trained network (also known as teacher) is transferred to a small student network (a.k.a.

---

\*Corresponding Author.

student) to enhance the performance of the latter. As an architecture-agnostic technique that can be effectively combined with other compression approaches to further boost model efficiency, knowledge distillation has emerged as a compelling and enduring focus in the field of efficient deep neural networks.

Hinton et al. [11] first propose distilling a teacher’s knowledge into a student by minimizing the Kullback-Leibler (KL) divergence between their logits. However, logit-based knowledge distillation methods fail to fully exploit the rich information encoded in the teacher network. To address this limitation, FitNet [13] introduces distillation using intermediate-layer features of the network. Subsequent feature-based distillation methods typically align features of the teacher and student networks by matching either one-to-one (or multi-pair) features holistically in the feature space, or align them after projecting them into alternative spaces [12, 14, 15]. However, in an individual global feature map, the distribution of semantic information across local regions is inherently uneven, and these local regions often exhibit varying degrees of interdependence. Such internal coupling imposes additional challenges to achieving effective and fine-grained feature distillation. Consequently, directly aligning global features between teacher and student networks tends to overlook the rich local information embedded within each feature map and the interdependencies among these local regions. This limitation hinders the student network’s ability to fully capture the “knowledge” from the teacher network, resulting in suboptimal performance.

To tackle these challenges, we propose a novel contrastive representation distillation framework called **MSDCRD** (see Figure 1), which integrates multi-scale feature decoupling with an efficient contrastive representation distillation strategy. Unlike CRD [16], which relies on extracting numerous feature samples from the entire dataset as negative samples, our method requires only a single mini-batch to generate abundant contrastive feature pairs via multi-scale feature decoupling. These pairs are derived not only from different data samples but also from diverse local regions within the same feature representation. Furthermore, the multi-scale decoupling strategy decouples the interdependencies among local regions within individual global features, thereby facilitating more effective knowledge transfer from the teacher network to the student network. Our method is completely parameter-free and plug-and-play, allowing flexible integration with various distillation strategies to further improve the performance of the student network.

Most existing feature-based distillation methods primarily focus on knowledge transfer between homogeneous models [13, 16, 17, 18, 19, 20], with only a few addressing the more challenging heterogeneous models [14, 21]. This is primarily because feature discrepancies are more pronounced in heterogeneous models than in homogeneous models. Further details can be found in Sec 5. Among the latter, methods that achieve relatively strong performance typically rely on projecting teacher and student features into alternative spaces prior to alignment, rather than aligning them directly in the original feature space. However, projecting features to alternative spaces may increase method complexity or hinder scalability across different tasks. In contrast to the aforementioned methods, our approach performs direct alignment in the feature space without relying on any auxiliary space mappings and achieves superior performance not only in homogeneous models but also across a wide range of heterogeneous teacher-student pairs. To demonstrate the superiority of our method, we conduct extensive experiments on multiple visual benchmarks under both homogeneous and heterogeneous models, highlighting the effectiveness of our approach as a flexible and architecture-agnostic feature distillation method. In summary, the main contributions of our work are as follows:

- We identify that existing feature distillation methods often overlook the interdependencies among local regions within individual feature maps, leading to suboptimal knowledge transfer. A multi-scale feature decoupling mechanism is introduced to decouple the interdependencies among local regions within individual feature maps, enabling the student to more effectively learn fine-grained knowledge from the teacher.
- We propose **MSDCRD**, a novel contrastive representation distillation method that integrates multi-scale feature decoupling with contrastive learning. Our method is parameter-free, plug-and-play, and exhibits strong generalization capability across diverse architectures and tasks.
- Extensive experiments are conducted on several visual benchmarks across both homogeneous and heterogeneous models. MSDCRD consistently enables significant performance improvements of student models across a variety of teacher-student architecture pairs, demonstrating its superior effectiveness.

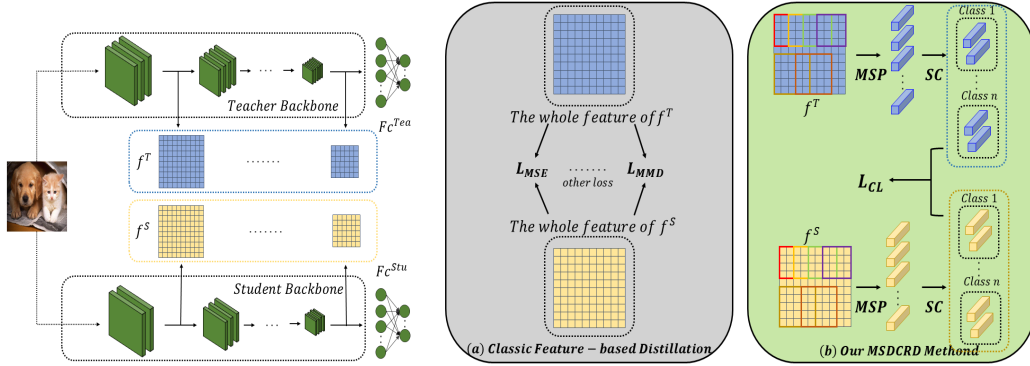


Figure 1: Illustration of Classic Feature-based Distillation and our MSDCRD method. (a) Classic Feature-based Distillation. Upon extracting features from the teacher and student networks, existing methods directly align the whole feature representations using different methods. (b) Our MSDCRD Method. Upon extracting feature representations from the teacher and student networks, we apply a multi-scale pooling (MSP) operation followed by sample categorization (SC) to systematically decouple the features across multiple semantic and spatial scales, a process referred to as multi-scale decoupling (MSD). The decoupled feature sample pairs are subsequently fed into our newly designed contrastive loss (CL) to facilitate fine-grained knowledge transfer. This figure is best viewed in color.

## 2 Related Work

Knowledge distillation transfers the “dark knowledge” of a complex teacher network to a lightweight student network, enhancing the performance of the student network. Knowledge distillation was first proposed by Hinton et al. [11], subsequent studies [22, 23, 24, 25, 26] have focused on developing diverse methodological advancements in the logit space for more effective knowledge transfer. Due to the inherent limitations of logit-based distillation and its inability to fully exploit the “knowledge” embedded in teacher networks, FitNet [13] first proposed distillation in the feature space. Since then, an increasing number of studies have focused on intermediate feature-based distillation [16, 17, 27, 18, 28, 19, 20, 21, 29, 14], as well as the emergence of attention-based distillation approaches [15, 12].

**Feature-Based Knowledge Distillation in Homogeneous Architectures.** Due to the strong task generality of feature-based distillation, an increasing number of researchers have proposed enhancements building upon the foundation established by FitNet [13]. PKT [20] aligned the probability distributions of teacher and student network features by minimizing their statistical divergence. OFD [18] distilled the features immediately preceding the final activation function at each stage of the network, and further proposed a novel activation function and a partial L2 loss to boost the performance of the student network. CRD [16] achieved efficient feature transfer by integrating knowledge distillation with contrastive learning. ReviewKD [27] improved knowledge distillation by introducing a review mechanism, in which the lower-layer features of the teacher guide the higher-layer features of the student. SimKD [17] achieved efficient knowledge transfer by directly reusing the teacher network’s classification layer as the student’s classifier.

**Feature-Based Knowledge Distillation in Heterogeneous Architectures.** In the past, CNN dominated as the mainstream architecture for visual tasks. However, models based on Transformer architectures [30, 31, 32] and MLP-based networks [33, 34] have recently emerged, demonstrating superior performance across various vision benchmarks. Due to the distinct inductive biases inherent to heterogeneous architectures, the feature representations produced by heterogeneous models also exhibit fundamental differences. As a result, knowledge transfer across heterogeneous models presents a more pronounced challenge compared to the case of homogeneous models. Most of the aforementioned feature-based distillation methods are primarily designed for homogeneous architectures, which may hinder their effectiveness when the teacher and student networks have different structures. Although there have been some studies [14, 21] that focus on feature-based distillation between heterogeneous models, the development of efficient, model-agnostic feature-based distillation techniques remains an open problem.

Existing feature-based distillation methods often overlook the significant semantic discrepancies among different local regions within an individual global feature representation, as well as the

coupling relationships between these local regions. To address this limitation, we propose a novel multi-scale feature decoupling mechanism for feature distillation, aiming to explicitly decouple the semantic interactions among local regions within an individual global feature representation. Furthermore, we integrate this strategy with a novel contrastive representation distillation framework, yielding a parameter-free and plug-and-play method that facilitates efficient knowledge transfer between teacher and student networks. Extensive experiments demonstrate that our method consistently achieves outstanding performance across both homogeneous and heterogeneous model architectures.

### 3 Method

As depicted in Figure 1, compared to previous feature-based distillation methods that directly align the global features of teacher and student networks, our proposed MSDCRD framework first introduces a multi-scale feature decoupling mechanism to explicitly decouple semantic dependencies between local regions within an individual global feature representation. The resulting decoupled feature sample pairs are then fed into a newly designed contrastive loss function, culminating in a novel, plug-and-play MSDCRD loss module.

**Notation.** Given a batch of input images of size  $B$ , denoted as  $x_i, x_j$  (where  $i, j = 1, 2, \dots, B$ ), with  $i = j$  indicating the same input image, we define  $f^S$  and  $f^T$  as the feature extractors of the student and teacher networks, respectively. Let the penultimate layer feature of the teacher network be represented as  $T^j = f^T(x_j) \in R^{c_T \times h_T \times w_T}$ , and the penultimate layer feature of the student network as  $f^S(x_i) \in R^{c_S \times h_S \times w_S}$ . The student’s feature is then passed through a projector to match the teacher’s channel dimension, denoted as  $S^i \in R^{c_T \times h_S \times w_S}$ . Here,  $c_T$  and  $c_S$  denote the number of feature channels for teacher and student networks, respectively, while  $h_T, w_T$  and  $h_S, w_S$  represent the spatial dimensions of teacher and student feature maps. The classifier of the teacher network, denoted as  $fc^T$ , first receives the global pooled representation of the feature map  $T^i$ , denoted as  $\bar{T}^i = GAP(T^i) \in R^{c_T \times 1 \times 1}$ , and then predicts the corresponding class label as  $C^i = fc^T(\bar{T}^i)$ .

#### 3.1 Multi-Scale Decoupling

For an individual global feature representation, different local regions typically encode diverse semantic information, with latent interdependencies often present among these local regions. Directly transferring the entire global feature during distillation may overlook the rich, diverse semantic information embedded within local regions of each feature map and fail to disentangle the inter-region couplings effectively. As a result, the student network may not fully capture the teacher’s knowledge, leading to suboptimal performance.

The multi-scale feature decoupling module designed for feature space primarily comprises two core stages: multi-scale pooling(MSP) and sample categorization(SC). In the MSP stage, feature maps are pooled at multiple spatial resolutions to capture diverse local semantics. Subsequently, the SC stage organizes these features into structured sample pairs based on spatial and semantic criteria, then categorizes them into three distinct types of sample pairs for contrastive learning.

**Multi-Scale Pooling.** We first extract the feature maps  $S^i$  and  $T^j$  from the student and teacher networks, respectively. To obtain multi-scale local features, we apply sliding-window pooling operations with varying kernel sizes and strides to each global feature map. This process yields a collection of pooled feature samples that correspond to local regions at varying spatial scales and positions within the global feature. These pooled samples are denoted as  $S_m^i \in R^{c_T \times 1 \times 1}$  and  $T_n^j \in R^{c_T \times 1 \times 1}$ , where  $m, n = 1, 2, \dots, M$ , and  $M$  denote the total number of pooled samples (including the globally pooled feature obtained via *GAP*) derived from an individual global feature. The condition  $m = n$  indicates that the pooled regions share the same pooling window size and position. When  $i = j$ , the teacher and student networks are fed with the same input image.

**Sample Categorization.** For each input image  $x_j$  fed into the teacher network, the extracted feature map  $T^j$  undergoes multi-scale pooling to produce  $M$  local feature samples, denoted as  $T_n^j$  for  $n = 1, 2, \dots, M$ . These features are then fed into the pretrained classifier  $fc^T$  of the teacher network to obtain the semantic category of each local region, yielding  $C_n^j = fc^T(T_n^j)$ . Given a single batch of  $B$  input images, MSP process yields  $B \times M$  pooled feature samples for both teacher and student networks. Each pooled feature sample from the teacher network is extracted from distinct spatial regions using multi-scale pooling across different input images. These localized features are

subsequently classified by the pretrained teacher classifier to obtain their corresponding semantic labels. The labeled local features are then used to construct student–teacher sample pairs based on their associated input image and pooling region. If  $C_m^i = C_n^j$ ,  $i = j$  and  $m = n$ , the student–teacher pair  $(S_m^i, T_n^j)$ , corresponding to the same input image and identical pooling region, is defined as a **related positive sample pair**. If  $C_m^i = C_n^j$ , but  $i \neq j$  or  $m \neq n$ , originating from different input images or distinct pooling regions but exhibiting similar semantic information, is considered an **other positive sample pair**. If  $C_m^i \neq C_n^j$ , and  $i \neq j$  or  $m \neq n$ , corresponding to different input images or spatial regions and possessing different semantic labels, is regarded as a **negative sample pair**.

### 3.2 Contrastive Loss

Compared to prior contrastive representation distillation [16], our method eliminates the reliance on a large memory bank that stores all feature representations from the teacher and student networks. Instead, it leverages only a single batch of inputs and, through the proposed multi-scale feature decoupling, generates a diverse set of rich feature samples with different semantic information. These samples are derived not only from different input images but also from distinct local regions within the same input.

For a batch of input data with size  $B$ , we can obtain  $B$  feature maps from the student and teacher networks, denoted as  $S^i$  and  $T^j$ , respectively. After applying multi-scale decoupling, each feature map yields  $M$  pooled local features, resulting in  $N = M \times B$  decoupled feature samples from each network, denoted as  $S_m^i$  and  $T_n^j$ . We would like to push closer the representations  $S_m^i$  and  $T_m^i$ , while pushing apart  $S_m^i$  and  $T_n^j$  (where  $i \neq j$  or  $m \neq n$ ). Specifically, we consider the joint distribution  $p(S_m^i, T_n^j)$  between the student network feature samples and the teacher network feature samples, as well as the product of the marginal distributions  $p(S_m^i)p(T_n^j)$ , and ultimately aim to maximize the mutual information between related positive sample pairs:

$$I(S_m^i, T_m^i) = E_{p(S_m^i, T_m^i)}(\log(\frac{p(S_m^i, T_m^i)}{p(S_m^i)p(T_m^i)})) \quad (1)$$

where  $E_{p(S_m^i, T_m^i)}(\cdot)$  indicates the expectation over related positive sample pairs,  $p(S_m^i, T_m^i)$  denotes the joint distribution of related positive sample pairs.

To achieve this goal, we define a distribution  $q$  and introduce a latent variable  $V$  that determines whether the distribution  $q$  for a given pair of student-teacher feature samples  $(S_m^i, T_n^j)$  is derived from the joint distribution  $p(S_m^i, T_n^j)$  or the product of the marginal distributions  $p(S_m^i)p(T_n^j)$ :

$$q(S_m^i, T_n^j | V = 1) = p(S_m^i, T_n^j) \quad (2)$$

$$q(S_m^i, T_n^j | V = 0) = p(S_m^i)p(T_n^j) \quad (3)$$

We set the latent variable  $V$  based on the three types of sample pairs obtained by applying the multi-scale feature decoupling described in Section 3.1. When  $i = j$  and  $m = n$ , the student-teacher feature pair is considered as a **related positive sample pair**. These features originate from the same input image, with identical pooling size and pooling position, making them highly correlated. Thus, we set  $V = 1$ . For the **other positive sample pairs**, although they share similar semantic information, the features are derived from different input images or different local regions; thus, they are treated as uncorrelated after applying MSD, and we set  $V = 0$ . For the **negative sample pairs**, the semantic content of the feature samples is inherently different, and they originate from different input images or distinct local regions, indicating no correlation. Accordingly, a value of  $V = 0$  is assigned.

The prior probability of the latent variable  $V$  can be easily derived as:

$$q(V = 1) = \frac{1}{N}, q(V = 0) = \frac{N - 1}{N} \quad (4)$$

According to Bayes' theorem, the posterior formula for the variable  $V$  can be written as:

$$\begin{aligned} q(V = 1 | S_m^i, T_n^j) &= \frac{q(S_m^i, T_n^j | V = 1)q(V = 1)}{q(S_m^i, T_n^j | V = 1)q(V = 1) + q(S_m^i, T_n^j | V = 0)q(V = 0)} \\ &= \frac{p(S_m^i, T_n^j)}{p(S_m^i, T_n^j) + (N - 1)p(S_m^i)p(T_n^j)} \end{aligned} \quad (5)$$

Taking the negative logarithm of both sides of Equation 5, and then applying the monotonicity of the logarithm function, we get:

$$\begin{aligned}
& -\log q(V = 1|S_m^i, T_n^j) \\
& = \log\left(1 + \frac{(N-1)p(S_m^i)p(T_n^j)}{p(S_m^i, T_n^j)}\right) \\
& \geq \log(N-1) - \log\left(\frac{p(S_m^i, T_n^j)}{p(S_m^i)p(T_n^j)}\right)
\end{aligned} \tag{6}$$

To maximize the mutual information between related positive sample pairs, we take the expectation on both sides of Equation 6 w.r.t.  $q(S_m^i, T_n^j|V = 1)$  (which is equivalent to  $p(S_m^i, T_n^j)$ , where  $i = j$  and  $m = n$ ). After rearranging, we obtain the form of Equation 1:

$$\begin{aligned}
& I(S_m^i, T_m^i) \\
& \geq \log(N-1) + E_{p(S_m^i, T_m^i)}(\log q(V = 1|S_m^i, T_m^i))
\end{aligned} \tag{7}$$

After removing the constant term on the right-hand side of Equation 7, we obtain the lower bound of mutual information between related positive sample pairs, denoted as *MI bound*.

$$MI \text{ bound} = E_{p(S_m^i, T_m^i)}(\log q(V = 1|S_m^i, T_m^i)) \tag{8}$$

Maximizing the lower bound *MI bound* is equivalent to maximizing  $I(S_m^i, T_m^i)$ , but since we cannot obtain the true distribution  $q(V = 1|S_m^i, T_n^j)$ , we construct an approximate distribution  $\tilde{q}(V = 1|S_m^i, T_n^j)$ , the formula is as follows:

$$\tilde{q}(V = 1|S_m^i, T_n^j) = \frac{\exp(\text{sim}(S_m^i, T_m^i))}{\sum_{j=1}^B \sum_{n=1}^M D(S_m^i, T_n^j)} \tag{9}$$

where  $\text{sim}(\cdot)$  is the cosine similarity function between two feature samples. Since other positive pairs may share similar semantic information, we mitigate this influence to achieve effective decoupling by employing a discriminator  $D(S_m^i, T_n^j)$  to suppress their impact.

$$D(S_m^i, T_n^j) = \begin{cases} 0, C_m^i = C_n^j, \text{ where } i \neq j \text{ or } m \neq n \\ \exp(\text{sim}(S_m^i, T_m^j)), \text{ otherwise} \end{cases} \tag{10}$$

Therefore, when maximizing Equation 11, it is equivalent to maximizing the mutual information between related positive sample pairs:

$$\max E_{p(S_m^i, T_m^i)}(\log \tilde{q}(V = 1|S_m^i, T_m^i)) \tag{11}$$

### 3.3 MSDCRD Loss

Due to the capacity gap, a lightweight student struggles to match the feature magnitude of a cumbersome teacher. Thus, we align the student's feature distribution with the teacher's as similar as possible. Therefore, before the feature samples are input into the loss function for calculation, we first perform L2 normalization. The final loss function of MSDCRD is formulated as follows:

$$L_{MSDCRD} = -\frac{1}{BM} \sum_{i=1}^B \sum_{m=1}^M \frac{\exp(\text{sim}(N(S_m^i), N(T_m^i)))}{\sum_{j=1}^B \sum_{n=1}^M D(N(S_m^i), N(T_n^j))} \tag{12}$$

where  $B$  represents the batch size,  $M$  denotes the number of distinct pooled feature maps obtained through multi-scale decoupling of an individual global feature,  $N(\cdot)$  applies L2 normalization, while  $\text{sim}(\cdot)$  computes the cosine similarity between two feature samples.  $D(\cdot, \cdot)$  as defined in Equation 10, serves as a discriminator to determine whether a student-teacher feature sample pair should be judged as an other positive sample pair.

Since  $L_{MSDCRD}$  is a plug-and-play module with no additional parameter requirements, it can be applied not only to the penultimate layer of the feature extractor's output but also extended to shallower layers of the network to achieve multi-layer feature distillation.

## 4 Experiments

We conduct extensive experiments across multiple tasks. First, we evaluate our method on the image classification task, performing both homogeneous and heterogeneous distillation on different datasets. The results demonstrate the superior performance of our approach and its architecture-agnostic nature. To further verify its generality, we also apply our method to other vision tasks. In all cases, the experimental results consistently show that our method brings significant performance improvements compared to other methods.

### 4.1 Classification

**Datasets.** We conduct experiments on CIFAR-100 [35] and ImageNet [36]. CIFAR-100 is a widely used image classification benchmark, containing 100 categories with 50,000 training images and 10,000 validation images, each with a resolution of 32×32. ImageNet is a larger-scale image classification dataset, consisting of images from 1,000 categories. The training set contains 1.28 million images, while the validation set includes 50,000 images.

**Implementation Details.** We perform both homogeneous and heterogeneous knowledge distillation experiments on CIFAR-100 and ImageNet. The implementation details are as follows:

On CIFAR-100, we conduct homogeneous distillation experiments using commonly adopted CNNs in visual tasks. We compare our method against several feature-based distillation approaches across multiple widely-used architectures, including VGG [37], ResNet [1], WideResNet [38], MobileNet [9], and ShuffleNet [39, 10]. We use the same training setting of [16]. For heterogeneous distillation experiments, we adopt three representative architectures in vision tasks: CNNs, Transformers, and MLPs. The detailed experimental settings are provided in the Appendix B.1. Each experiment is run three times, and we report the average top-1 accuracy.

On ImageNet, we also perform homogeneous distillation experiments using popular CNN architectures, comparing our method with recent feature-based distillation approaches. For heterogeneous distillation experiments, we adopt the same three architectures: CNNs, Transformers, and MLPs. The detailed experimental settings are provided in the Appendix B.1. Each experiment is run three times, and we report the average top-1 accuracy.

**Results on Homogeneous Models.** On CIFAR-100, we categorize existing methods into three groups based on the space in which distillation is performed: logits-based [11, 26, 23], attention-based [12, 15], and feature-based [13, 28, 16, 17, 18, 27, 40, 41] approaches. Table 1 and Table 2 present comparisons involving only a subset of teacher-student pairs and selected representative methods. Specifically, Table 1 reports results for pairs with the same architectural style, while Table 2 focuses on pairs with different architectural styles. These results indicate that MSDCRD consistently achieves state-of-the-art performance in most cases and demonstrates comprehensive improvements over the conventional CRD. Notably, MSDCRD enables several student models to surpass their teachers in performance. Comprehensive comparisons and detailed analysis can be found in the Appendix B.2.

Table 1: **Selected Results on CIFAR-100.** Homogeneous distillation results with **identical** Teacher-Student architectures. The best and second-best results are emphasized in **bold** and underlined cases.

Teacher	Student	From Scratch		Logits-based		Attention-based		Feature-based				Feature-based	
		T.	S.	KD		AT	CAT-KD	FitNet	RKD	SimKD	OFD	ReviewKD	CRD
ResNet110	ResNet32	74.31	71.14	73.08	72.31	73.62	71.06	71.82	<u>73.92</u>	73.23	73.89	73.48	<b>74.61</b> (↑+1.13)
WRN-40-2	WRN-16-2	75.61	73.26	74.92	74.08	75.60	73.58	73.35	75.53	75.24	<u>76.12</u>	75.48	<b>76.66</b> (↑+1.18)
ResNet32×4	ResNet8×4	79.42	72.50	73.33	73.44	76.91	73.50	71.90	<b>78.08</b>	74.95	75.63	75.51	<u>77.43</u> (↑+1.92)
VGG13	VGG8	74.64	70.36	72.98	71.43	74.65	71.02	71.48	<u>74.89</u>	73.95	74.84	73.94	<b>75.65</b> (↑+1.71)

Table 2: **Selected Results on CIFAR-100.** Homogeneous distillation results with **distinct** Teacher-Student architectures. The best and second-best results are emphasized in **bold** and underlined cases.

Teacher	Student	From Scratch		Logits-based		Attention-based		Feature-based				Feature-based	
		T.	S.	KD		AT	CAT-KD	FitNet	RKD	SimKD	OFD	ReviewKD	CRD
ResNet32×4	WRN-40-2	79.42	75.61	77.70	77.43	78.59	77.69	77.82	<u>79.29</u>	79.25	78.96	78.15	<b>80.34</b> (↑+2.19)
ResNet32×4	ShuffleNetV1	79.42	70.50	74.07	71.73	<u>78.26</u>	73.59	72.28	77.18	75.98	77.45	75.11	<b>78.65</b> (↑+3.54)
WRN-40-2	ResNet8×4	75.61	72.50	73.97	74.11	<u>75.38</u>	74.61	75.26	75.29	74.36	74.34	75.24	<b>76.93</b> (↑+1.69)
ResNet50	MobileNetV2	79.34	64.60	67.35	58.58	<u>71.36</u>	63.16	64.43	69.97	69.04	69.89	69.11	<b>71.51</b> (↑+2.40)

On ImageNet, we follow the same categorization protocol as in CIFAR-100, dividing baseline methods into logits-based, attention-based, and feature-based distillation strategies. We experiment with two settings of distillation from ResNet50 to MobileNet, and from ResNet34 to ResNet18 respectively. Table 3 shows that our method consistently surpasses all competing approaches, regardless of whether

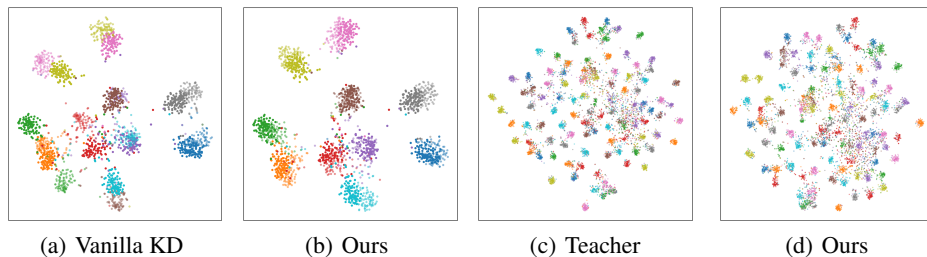


Figure 2: Visualization results of test images from CIFAR-100 with t-SNE. In (a) and (b), we randomly sample 10 out of the 100 classes. The features extracted by the teacher and student models are represented in dark and light colors, respectively, and in our method, they are nearly indistinguishable. In (c) and (d), we present the visualizations of all classes for the teacher and the student trained with **MSDCRD**. This figure is best viewed in color.

the teacher and student share the identical architecture or not. This further verifies the robustness and generalizability of our method under homogeneous models.

Table 3: **Results on ImageNet**. The best results are emphasized in **bold** cases.

Teacher	Student		From Scratch		Logits-based	Attention-based		Feature-based			Feature-based	
			T.	S.	KD	AT	CAT-KD	SimKD	OFD	ReviewKD	CRD	<b>MSDCRD</b>
ResNet32	ResNet18	Top-1	73.31	69.75	71.03	70.69	71.26	71.59	70.81	71.61	71.17	<b>71.99</b>
		Top-5	91.42	89.07	90.05	90.01	90.45	90.48	89.98	90.51	90.13	<b>90.52</b>
ResNet50	MobileNet	Top-1	76.16	68.87	70.05	69.56	72.24	72.25	71.25	72.56	71.37	<b>73.06</b>
		Top-5	92.86	88.76	89.80	89.33	91.13	90.86	90.34	91.00	90.41	<b>91.15</b>

**Results on Heterogeneous Models.** On CIFAR-100, we categorize heterogeneous distillation experiments into two groups following the same grouping criteria adopted in the homogeneous setting. Specifically, we conduct comprehensive cross-architecture distillation among three heterogeneous model families: CNNs, Transformers, and MLPs, to evaluate the effectiveness of our method under heterogeneous conditions. As shown in Table 4 and Table 5, our method achieves SOTA performance across a wide range of heterogeneous architectures by performing alignment solely in the feature space. Compared to traditional feature-based distillation methods such as CRD, it yields substantial performance gains, highlighting the robustness and efficacy of our approach in heterogeneous settings. More detailed analysis can be found in the Appendix B.3.

Table 4: **Results on CIFAR-100**. Distillation between heterogeneous Teacher-Student models. The best and second-best results are emphasized in **bold** and underlined cases.

Teacher	Student	From Scratch		Logits-based				Feature-based			Feature-based	
		T.	S.	KD	DKD	DIST	OFAKD	FitNet	CC	RKD	CRD	<b>MSDCRD</b>
Swin-T	ResNet18	89.26	74.01	78.74	80.26	77.75	<u>80.54</u>	78.87	74.19	74.11	77.63	<b>82.75</b> ( $\uparrow+5.12$ )
ViT-S	ResNet18	92.04	74.01	77.26	78.10	76.49	<u>80.15</u>	77.71	74.26	73.72	76.60	<b>81.93</b> ( $\uparrow+5.44$ )
Mixer-B/16	ResNet18	87.29	74.01	77.79	78.67	76.36	<b>79.39</b>	77.15	74.26	73.75	76.42	<u>79.26</u> ( $\uparrow+2.54$ )
ConvNeXt-T	DeiT-T	88.41	68.00	72.99	74.60	73.55	<u>75.76</u>	60.78	68.01	69.79	65.94	<b>85.52</b> ( $\uparrow+19.58$ )
ConvNeXt-T	Swin-P	88.41	72.63	76.44	76.80	76.41	<u>78.32</u>	24.06	72.63	71.73	67.09	<b>84.7</b> ( $\uparrow+17.61$ )
Mixer-B/16	DeiT-T	87.29	68.00	71.36	73.44	71.67	<u>73.90</u>	71.05	68.13	69.89	65.35	<b>81.18</b> ( $\uparrow+15.83$ )
Mixer-B/16	Swin-P	87.29	72.63	75.93	76.39	75.85	<u>78.93</u>	75.20	73.32	70.82	67.03	<b>79.46</b> ( $\uparrow+12.43$ )
ConvNeXt-T	ResMLP-S12	88.41	66.56	72.25	73.22	71.93	<u>81.22</u>	45.47	67.70	65.82	63.35	<b>87.21</b> ( $\uparrow+23.86$ )
Swin-T	ResMLP-S12	87.29	66.56	71.89	72.82	11.05	<u>80.63</u>	63.12	68.37	64.66	61.72	<b>86.45</b> ( $\uparrow+24.73$ )

On ImageNet, we similarly conduct heterogeneous distillation experiments across the three architectural families, following the same grouping protocol as in previous settings. Our method achieves SOTA performance in the majority of cases. Notably, compared to strong methods such as OFAKD and FitNet, our approach relies solely on single-layer feature alignment within the feature space. Despite the substantial discrepancies in feature representations across heterogeneous models, the results demonstrate that our method is still able to facilitate effective knowledge transfer. More detailed analysis can be found in the Appendix B.3.

## 4.2 Object Detection

To further evaluate the extensibility of our method, we apply MSDCRD to additional vision tasks. In the object detection task, the backbone features of the teacher network are distilled into the student network. We conduct experiments on the representative COCO2017 dataset [42] using the widely adopted Detectron2 framework [43] as our strong baseline. The comparison results are summarized in Table 6. Further implementation details, comprehensive analysis, and additional experimental results are provided in the Appendix. C

Table 5: **Results on ImageNet.** Distillation between heterogeneous Teacher-Student models. The best and second-best results are emphasized in **bold** and underlined cases.

Teacher	Student	From Scratch		Logits-based				Feature-based			Feature-based	
		T.	S.	KD	DKD	DIST	OFAKD	FitNet	CC	RKD	CRD	<b>MSDCRD</b>
Swin-T	ResNet18	81.38	69.75	71.14	71.10	70.91	<u>71.85</u>	71.18	70.07	69.47	69.25	<b>71.92</b> ( $\uparrow+2.67$ )
Mixer-B/16	ResNet18	76.62	69.75	<u>70.89</u>	69.89	70.66	<b>71.38</b>	70.78	70.05	69.46	68.40	70.10( $\uparrow+1.70$ )
ConvNeXt-T	Swin-N	82.05	75.53	77.15	77.00	77.25	<u>77.50</u>	74.81	75.79	75.48	74.15	<b>77.61</b> ( $\uparrow+3.46$ )
Mixer-B/16	Swin-N	76.62	75.53	76.26	75.03	<u>76.54</u>	<b>76.63</b>	76.17	75.81	75.52	73.38	75.68( $\uparrow+2.30$ )
ConvNeXt-T	ResMLP-S12	82.05	76.65	76.84	77.23	77.24	<u>77.53</u>	74.69	75.79	75.28	73.57	<b>78.29</b> ( $\uparrow+4.72$ )
Swin-T	ResMLP-S12	81.38	76.65	76.67	76.99	77.25	<u>77.31</u>	76.48	76.15	75.10	73.40	<b>77.53</b> ( $\uparrow+4.13$ )

Table 6: **Results on object detection.** We use AP on different settings to evaluate results. “R101” denotes the use of ResNet-101 as backbone, and the same naming convention applies to other models.

Method		mAP	AP50	AP75	API	APm	APS
Teacher	Faster R-CNN w/ R101-FPN	42.04	62.48	45.88	54.60	45.55	25.22
Student	Faster R-CNN w/ R50-FPN	37.93	58.84	41.05	49.10	41.14	22.44
	w/ KD	38.35 (+0.42)	59.41	41.71	49.48	41.80	22.73
	w/ FitNet	38.76 (+0.83)	59.62	41.80	50.70	42.20	22.32
	w/ FIGI	39.44 (+1.51)	60.27	43.04	<b>51.97</b>	42.51	22.89
	w/ MSDCRD	<b>39.65</b> (+1.72)	<b>60.28</b>	<b>43.22</b>	51.63	<b>43.38</b>	<b>23.43</b>

## 5 Extension Experiments

**Feature visualizations.** As shown in Figure 2(b), the features extracted by the teacher model (dark colors) and the student model distilled using MSDCRD(light colors) form tight clusters within the same class and are clearly separated across different classes, while closely aligning with the teacher network’s features. Figure 2(c) and Figure 2(d) visualize the feature maps of all classes from the pre-trained teacher network and the student network trained with MSDCRD, respectively. It is evident that our approach achieves performance comparable to the teacher network. (In fact, the student network trained with MSDCRD outperforms the teacher network in actual results.) This demonstrates the effectiveness of our method in transferring knowledge from teacher to student.

**Ablation Study.** To validate the effectiveness of each component proposed in Section 3, we conduct an ablation study by incrementally incorporating them into the baseline. The results are shown in Table 7, we conduct each experiment three times and report the average accuracy. We use ResNet8 $\times$ 4 as the student network and ResNet32 $\times$ 4 as the teacher network, with CRD serving as our baseline. Introducing the CL module that operates using only single batch samples alone, already surpasses the baseline. Further adding the MSP and SC modules from Section 3.1 leads to consistent performance gains, ultimately achieving the best results.

Table 7: **Ablation study.** CL: our designed contrastive loss function. Multi-Scale Decoupling (MSD) is decomposed into two modules: Multi-Scale Pooling (MSP) and Sample Categorization (SC).

CL	MSD		Accuracy
	MSP	SC	
			75.48
✓			76.44
✓	✓		77.10
✓	✓	✓	<b>77.43</b>

**Feature discrepancies between homogeneous and heterogeneous models.** To explicitly illustrate the discrepancies in feature representations across different network architectures, we compare the feature similarity between layers of various models. To this end, we adopt the centered kernel alignment (CKA) metric to quantify these differences. More detailed analysis provided in the Appendix D The results ultimately show that, compared to homogeneous models, heterogeneous models exhibit more pronounced discrepancies in the feature space. Despite these challenges, our proposed MSDCRD framework not only achieves strong performance in homogeneous models with either similar or distinct architectural styles but also enables effective knowledge transfer in the more challenging heterogeneous models, demonstrating its strong generalizability in feature-based distillation.

## 6 Conclusion and Future Work

In this work, we first identify a key limitation of existing feature-based distillation methods: the inability to effectively decouple interdependent local regions within an individual global feature. To address this, we propose a novel framework called MSDCRD, which performs multi-scale decoupling on individual feature maps and combines it with a newly designed contrastive loss. Extensive experiments across various visual tasks validate the superior performance of our approach. In addition, MSDCRD is a parameter-free and plug-and-play method, making it highly flexible and easily adaptable to a wide range of advanced distillation strategies for further performance improvement. This design suggests promising potential for future research.

## References

- [1] Kaiming He, Xiangyu Zhang, Shaoqing Ren, and Jian Sun. Deep residual learning for image recognition. In *Proceedings of the IEEE conference on computer vision and pattern recognition*, pages 770–778, 2016.
- [2] Jonathan Frankle and Michael Carbin. The lottery ticket hypothesis: Finding sparse, trainable neural networks. *arXiv preprint arXiv:1803.03635*, 2018.
- [3] Hao Li, Asim Kadav, Igor Durdanovic, Hanan Samet, and Hans Peter Graf. Pruning filters for efficient convnets. *arXiv preprint arXiv:1608.08710*, 2016.
- [4] Zhuang Liu, Mingjie Sun, Tinghui Zhou, Gao Huang, and Trevor Darrell. Rethinking the value of network pruning. *arXiv preprint arXiv:1810.05270*, 2018.
- [5] Jian-Hao Luo, Jianxin Wu, and Weiyao Lin. Thinet: A filter level pruning method for deep neural network compression. In *Proceedings of the IEEE international conference on computer vision*, pages 5058–5066, 2017.
- [6] Benoit Jacob, Skirmantas Kligys, Bo Chen, Menglong Zhu, Matthew Tang, Andrew Howard, Hartwig Adam, and Dmitry Kalenichenko. Quantization and training of neural networks for efficient integer-arithmetic-only inference. In *Proceedings of the IEEE conference on computer vision and pattern recognition*, pages 2704–2713, 2018.
- [7] Matthieu Courbariaux, Yoshua Bengio, and Jean-Pierre David. Binaryconnect: Training deep neural networks with binary weights during propagations. *Advances in neural information processing systems*, 28, 2015.
- [8] Andrew G Howard. Mobilenets: Efficient convolutional neural networks for mobile vision applications. *arXiv preprint arXiv:1704.04861*, 2017.
- [9] Mark Sandler, Andrew Howard, Menglong Zhu, Andrey Zhmoginov, and Liang-Chieh Chen. Mobilenetv2: Inverted residuals and linear bottlenecks. In *Proceedings of the IEEE conference on computer vision and pattern recognition*, pages 4510–4520, 2018.
- [10] Xiangyu Zhang, Xinyu Zhou, Mengxiao Lin, and Jian Sun. Shufflenet: An extremely efficient convolutional neural network for mobile devices. In *Proceedings of the IEEE conference on computer vision and pattern recognition*, pages 6848–6856, 2018.
- [11] Geoffrey Hinton. Distilling the knowledge in a neural network. *arXiv preprint arXiv:1503.02531*, 2015.
- [12] Sergey Zagoruyko and Nikos Komodakis. Paying more attention to attention: Improving the performance of convolutional neural networks via attention transfer. *arXiv preprint arXiv:1612.03928*, 2016.
- [13] Adriana Romero, Nicolas Ballas, Samira Ebrahimi Kahou, Antoine Chassang, Carlo Gatta, and Yoshua Bengio. Fitnets: Hints for thin deep nets. *arXiv preprint arXiv:1412.6550*, 2014.
- [14] Zhiwei Hao, Jianyuan Guo, Kai Han, Yehui Tang, Han Hu, Yunhe Wang, and Chang Xu. One-for-all: Bridge the gap between heterogeneous architectures in knowledge distillation. *Advances in Neural Information Processing Systems*, 36:79570–79582, 2023.
- [15] Ziyao Guo, Haonan Yan, Hui Li, and Xiaodong Lin. Class attention transfer based knowledge distillation. In *Proceedings of the IEEE/CVF Conference on Computer Vision and Pattern Recognition*, pages 11868–11877, 2023.
- [16] Yonglong Tian, Dilip Krishnan, and Phillip Isola. Contrastive representation distillation. *arXiv preprint arXiv:1910.10699*, 2019.
- [17] Defang Chen, Jian-Ping Mei, Hailin Zhang, Can Wang, Yan Feng, and Chun Chen. Knowledge distillation with the reused teacher classifier. In *Proceedings of the IEEE/CVF conference on computer vision and pattern recognition*, pages 11933–11942, 2022.

- [18] Byeongho Heo, Jeessoo Kim, Sangdoon Yun, Hyojin Park, Nojun Kwak, and Jin Young Choi. A comprehensive overhaul of feature distillation. In *Proceedings of the IEEE/CVF international conference on computer vision*, pages 1921–1930, 2019.
- [19] Sungsoo Ahn, Shell Xu Hu, Andreas Damianou, Neil D Lawrence, and Zhenwen Dai. Variational information distillation for knowledge transfer. In *Proceedings of the IEEE/CVF conference on computer vision and pattern recognition*, pages 9163–9171, 2019.
- [20] Nikolaos Passalis, Maria Tzelepi, and Anastasios Tefas. Probabilistic knowledge transfer for lightweight deep representation learning. *IEEE Transactions on Neural Networks and Learning Systems*, 32(5):2030–2039, 2020.
- [21] Junjie Zhou, Ke Zhu, and Jianxin Wu. All you need in knowledge distillation is a tailored coordinate system. In *Proceedings of the AAAI Conference on Artificial Intelligence*, volume 39, pages 22946–22954, 2025.
- [22] Shicai Wei Chunbo Luo Yang Luo. Scale decoupled distillation. *arXiv preprint arXiv:2403.13512*, 2024.
- [23] Borui Zhao, Quan Cui, Renjie Song, Yiyu Qiu, and Jiajun Liang. Decoupled knowledge distillation. In *Proceedings of the IEEE/CVF Conference on computer vision and pattern recognition*, pages 11953–11962, 2022.
- [24] Shangquan Sun, Wenqi Ren, Jingzhi Li, Rui Wang, and Xiaochun Cao. Logit standardization in knowledge distillation. In *Proceedings of the IEEE/CVF Conference on Computer Vision and Pattern Recognition*, pages 15731–15740, 2024.
- [25] Ying Jin, Jiaqi Wang, and Dahua Lin. Multi-level logit distillation. In *Proceedings of the IEEE/CVF Conference on Computer Vision and Pattern Recognition*, pages 24276–24285, 2023.
- [26] Zheng Li, Xiang Li, Lingfeng Yang, Borui Zhao, Renjie Song, Lei Luo, Jun Li, and Jian Yang. Curriculum temperature for knowledge distillation. In *Proceedings of the AAAI Conference on Artificial Intelligence*, volume 37, pages 1504–1512, 2023.
- [27] Pengguang Chen, Shu Liu, Hengshuang Zhao, and Jiaya Jia. Distilling knowledge via knowledge review. In *Proceedings of the IEEE/CVF conference on computer vision and pattern recognition*, pages 5008–5017, 2021.
- [28] Wonpyo Park, Dongju Kim, Yan Lu, and Minsu Cho. Relational knowledge distillation. In *Proceedings of the IEEE/CVF conference on computer vision and pattern recognition*, pages 3967–3976, 2019.
- [29] Yuzhu Wang, Lechao Cheng, Manni Duan, Yongheng Wang, Zunlei Feng, and Shu Kong. Improving knowledge distillation via regularizing feature direction and norm. In *European Conference on Computer Vision*, pages 20–37. Springer, 2024.
- [30] Alexey Dosovitskiy, Lucas Beyer, Alexander Kolesnikov, Dirk Weissenborn, Xiaohua Zhai, Thomas Unterthiner, Mostafa Dehghani, Matthias Minderer, Georg Heigold, Sylvain Gelly, et al. An image is worth 16x16 words: Transformers for image recognition at scale. *arXiv preprint arXiv:2010.11929*, 2020.
- [31] Ze Liu, Yutong Lin, Yue Cao, Han Hu, Yixuan Wei, Zheng Zhang, Stephen Lin, and Baining Guo. Swin transformer: Hierarchical vision transformer using shifted windows. In *Proceedings of the IEEE/CVF international conference on computer vision*, pages 10012–10022, 2021.
- [32] Hugo Touvron, Matthieu Cord, Matthijs Douze, Francisco Massa, Alexandre Sablayrolles, and Hervé Jégou. Training data-efficient image transformers & distillation through attention. In *International conference on machine learning*, pages 10347–10357. PMLR, 2021.
- [33] Hugo Touvron, Piotr Bojanowski, Mathilde Caron, Matthieu Cord, Alaaeldin El-Nouby, Edouard Grave, Gautier Izacard, Armand Joulin, Gabriel Synnaeve, Jakob Verbeek, et al. Resmlp: Feedforward networks for image classification with data-efficient training. *IEEE transactions on pattern analysis and machine intelligence*, 45(4):5314–5321, 2022.

- [34] Ilya O Tolstikhin, Neil Houlsby, Alexander Kolesnikov, Lucas Beyer, Xiaohua Zhai, Thomas Unterthiner, Jessica Yung, Andreas Steiner, Daniel Keysers, Jakob Uszkoreit, et al. Mlp-mixer: An all-mlp architecture for vision. *Advances in neural information processing systems*, 34:24261–24272, 2021.
- [35] Alex Krizhevsky, Geoffrey Hinton, et al. Learning multiple layers of features from tiny images. 2009.
- [36] Olga Russakovsky, Jia Deng, Hao Su, Jonathan Krause, Sanjeev Satheesh, Sean Ma, Zhiheng Huang, Andrej Karpathy, Aditya Khosla, Michael Bernstein, et al. Imagenet large scale visual recognition challenge. *International journal of computer vision*, 115:211–252, 2015.
- [37] Karen Simonyan. Very deep convolutional networks for large-scale image recognition. *arXiv preprint arXiv:1409.1556*, 2014.
- [38] Sergey Zagoruyko. Wide residual networks. *arXiv preprint arXiv:1605.07146*, 2016.
- [39] Ningning Ma, Xiangyu Zhang, Hai-Tao Zheng, and Jian Sun. Shufflenet v2: Practical guidelines for efficient cnn architecture design. In *Proceedings of the European conference on computer vision (ECCV)*, pages 116–131, 2018.
- [40] Xueqing Deng, Dawei Sun, Shawn Newsam, and Peng Wang. Distpro: Searching a fast knowledge distillation process via meta optimization. In *European Conference on Computer Vision*, pages 218–235. Springer, 2022.
- [41] Xiaolong Liu, Lujun Li, Chao Li, and Anbang Yao. Norm: Knowledge distillation via n-to-one representation matching. *arXiv preprint arXiv:2305.13803*, 2023.
- [42] Tsung-Yi Lin, Michael Maire, Serge Belongie, James Hays, Pietro Perona, Deva Ramanan, Piotr Dollár, and C Lawrence Zitnick. Microsoft coco: Common objects in context. In *Computer vision—ECCV 2014: 13th European conference, zurich, Switzerland, September 6-12, 2014, proceedings, part v 13*, pages 740–755. Springer, 2014.
- [43] Yuxin Wu, Alexander Kirillov, Francisco Massa, Wan-Yen Lo, and Ross Girshick. Detectron2. 2019.
- [44] Vaishnavh Nagarajan, Aditya K Menon, Srinadh Bhojanapalli, Hossein Mobahi, and Sanjiv Kumar. On student-teacher deviations in distillation: does it pay to disobey? *Advances in Neural Information Processing Systems*, 36:5961–6000, 2023.
- [45] Tao Wang, Li Yuan, Xiaopeng Zhang, and Jiashi Feng. Distilling object detectors with fine-grained feature imitation. In *Proceedings of the IEEE/CVF conference on computer vision and pattern recognition*, pages 4933–4942, 2019.
- [46] Shaoqing Ren, Kaiming He, Ross Girshick, and Jian Sun. Faster r-cnn: Towards real-time object detection with region proposal networks. *Advances in neural information processing systems*, 28, 2015.
- [47] Tsung-Yi Lin, Priya Goyal, Ross Girshick, Kaiming He, and Piotr Dollár. Focal loss for dense object detection. In *Proceedings of the IEEE international conference on computer vision*, pages 2980–2988, 2017.
- [48] Corinna Cortes, Mehryar Mohri, and Afshin Rostamizadeh. Algorithms for learning kernels based on centered alignment. *The Journal of Machine Learning Research*, 13(1):795–828, 2012.
- [49] Simon Kornblith, Mohammad Norouzi, Honglak Lee, and Geoffrey Hinton. Similarity of neural network representations revisited. In *International conference on machine learning*, pages 3519–3529. PMLR, 2019.

## A Technical Appendices and Supplementary Material

### B Classification

#### B.1 Implementation Details

For homogeneous models, we adopt mainstream CNN architectures commonly used in visual tasks. For heterogeneous models, we employ several widely adopted backbone architectures in modern vision tasks, including CNNs, Transformers, and MLPs. The detailed experimental setups are described as follows:

**CIFAR-100.** For homogeneous model experiments, we train all models for 240 epochs, applying a learning rate decay of 0.1 every 30 epochs after the initial 150 epochs. The batch size is set to 64 for each model.

For heterogeneous model experiments, since ViTs and MLPs accept image patches as input, CIFAR-100 images are upsampled to a resolution of 224×224 for all heterogeneous experiments. All models are trained for 300 epochs. CNN-based students are optimized using SGD, while Transformer- and MLP-based students are trained using the AdamW optimizer.

All the aforementioned experiments on both homogeneous and heterogeneous models based on the CIFAR-100 dataset are conducted on a single NVIDIA 3090 GPU.

**ImageNet.** For homogeneous model experiments, we follow a standard training protocol: all models are trained for 100 epochs with an initial learning rate of 0.1, which is decayed by a factor of 0.1 every 30 epochs.

For heterogeneous model experiments, CNN-based students are trained for 100 epochs using the SGD optimizer, while Transformer- and MLP-based students are trained for 300 epochs using the AdamW optimizer.

All the aforementioned homogeneous and heterogeneous experiments on the ImageNet dataset are conducted using four NVIDIA 3090 GPUs.

#### B.2 Results on Homogeneous Models.

Table 8 and Table 9 present a more comprehensive set of comparison results on CIFAR-100 under homogeneous models. We introduce a wider range of teacher–student pairs and incorporate additional baseline methods to further highlight the effectiveness of our proposed MSDCRD.

For logits-based distillation, we use the classic KD [11] method as well as the more advanced CTKD [26] and DKD [23] methods. For attention-based distillation, we use AT [12] and CAT-KD [15]. For feature-based distillation, we compare with several widely-used and cutting-edge approaches, including FitNet [13], RKD [28], CRD [16], SimKD [17], OFD [18], ReviewKD [27], DistPro [40], and NORM [41].

It is evident that MSDCRD consistently demonstrates superior performance, regardless of whether the teacher and student networks have architectures of the same style or different architectures. Compared to the traditional CRD, our method achieves comprehensive improvements ranging from 0.36% to 3.54% across various teacher–student pairs.

Notably, in several teacher–student pairs such as ResNet32×4 → WRN-40-2 and ResNet110 → ResNet32, the students even outperform their teachers. This finding contradicts the previous empirical belief that the student network should merely mimic the distribution of the teacher network as closely as possible. Some studies, such as [44], suggest that this phenomenon is possible because the student does not simply mimic the teacher’s predictions but learns from a systematic bias in the teacher’s distribution. Such bias, induced by the regularization effect of knowledge distillation, tends to amplify high-confidence predictions while suppressing low-confidence ones. This introduces a denoising effect that enhances generalization capabilities, enabling the student network to surpass the performance of its teacher.

Table 8: **Comprehensive Results on CIFAR-100.** Homogeneous distillation results with **identical** Teacher-Student architectures. The best and second-best results are emphasized in **bold** and underlined cases. We mark the results where our method outperforms the teacher network with **\***.

	Teacher	ResNet110	ResNet110	ResNet56	ResNet32×4	WRN-40-2	WRN-40-2	VGG13
Type	Acc	74.31	74.31	72.34	79.42	75.61	75.61	74.64
	Student	ResNet32	ResNet20	ResNet20	ResNet8×4	WRN-16-2	WRN-40-1	VGG8
	Acc	71.14	69.06	69.06	72.50	73.26	71.98	70.36
Logit	KD	73.08	70.67	70.66	73.33	74.92	73.54	72.98
	CTKD	73.52	70.99	71.19	73.39	75.45	73.93	73.52
	DKD	<u>74.11</u>	71.06	<u>71.97</u>	76.32	76.24	74.81	74.68
Attention	AT	72.31	70.65	70.55	73.44	74.08	72.77	71.43
	CAT-KD	73.62	71.37	71.62	76.91	75.60	74.82	74.65
Feature	FitNet	71.06	68.99	69.21	73.50	73.58	72.24	71.02
	RKD	71.82	69.25	69.61	71.90	73.35	72.22	71.48
	SimKD	73.92	71.06	71.05	<b>78.08</b>	75.53	74.53	<u>74.89</u>
	OFD	73.23	71.29	70.98	74.95	75.24	74.33	73.95
	ReviewKD	73.89	71.34	71.89	75.63	76.12	75.09	74.84
	DistPro	73.74	n/a	<b>72.03</b>	n/a	<u>76.36</u>	<u>75.56</u>	n/a
	NORM	73.67	<u>71.55</u>	71.35	76.98	76.26	74.82	74.46
Feature	CRD	73.48	71.46	71.16	75.51	75.48	74.14	73.94
	<b>MSDCRD</b>	<b>*74.61</b>	<b>72.05</b>	71.46	<u>77.43</u>	<b>*76.66</b>	<b>*75.75</b>	<b>*75.65</b>
	↑	+1.13	+0.59	+0.36	+1.92	+1.18	+1.61	+1.71

Table 9: **Comprehensive Results on CIFAR-100.** Homogeneous distillation results with **distinct** Teacher-Student architectures. The best and second-best results are emphasized in **bold** and underlined cases. We mark the results where our method outperforms the teacher network with **\***.

	Teacher	ResNet32×4	ResNet32×4	ResNet32×4	ResNet32×4	WRN-40-2	VGG13	ResNet50
Type	Acc	79.42	79.42	79.42	79.42	75.61	74.64	79.34
	Student	ShuffleNetV1	ShuffleNetV2	WRN-40-2	WRN-16-2	ResNet8×4	MobileNetV2	MobileNetV2
	Acc	70.50	71.82	75.61	73.26	72.50	64.60	64.60
Logit	KD	74.07	74.45	77.70	74.90	73.97	67.37	67.35
	CTKD	74.48	75.37	77.66	74.57	74.61	68.50	68.67
	DKD	76.45	77.07	78.46	75.70	75.56	69.71	70.35
Attention	AT	71.73	72.73	77.43	73.91	74.11	59.40	58.58
	CAT-KD	<u>78.26</u>	<u>78.41</u>	78.59	76.97	<u>75.38</u>	69.13	<u>71.36</u>
Feature	FitNet	73.59	73.54	77.69	74.70	74.61	64.16	63.16
	RKD	72.28	73.21	77.82	74.86	75.26	64.52	64.43
	SimKD	77.18	78.39	<u>79.29</u>	<u>77.17</u>	75.29	69.44	69.97
	OFD	75.98	76.82	79.25	76.17	74.36	69.48	69.04
	ReviewKD	77.45	77.78	78.96	76.11	74.34	<u>70.37</u>	69.89
	DistPro	77.18	77.54	n/a	n/a	n/a	n/a	n/a
	NORM	77.42	78.32	n/a	n/a	n/a	68.94	70.56
Feature	CRD	75.11	75.65	78.15	75.65	75.24	69.73	69.11
	<b>Ours</b>	<b>78.65</b>	<b>78.67</b>	<b>*80.34</b>	<b>77.48</b>	<b>*76.93</b>	<b>70.47</b>	<b>71.51</b>
	↑	+3.54	+3.02	+2.19	+1.83	+1.69	+0.74	+2.40

### B.3 Results on Heterogeneous Models.

From the performance comparisons on both Table 4 and Table 5, it is evident that while traditional CRD struggles in heterogeneous models. In contrast, our proposed MSDCRD not only achieves superior results in homogeneous models but also consistently demonstrates outstanding performance across heterogeneous teacher-student pairs, significantly outperforming conventional CRD.

Given the substantial discrepancies in feature representations among heterogeneous models D, some recent methods (e.g., OFAKD) attempt to map features into alternative spaces for better alignment. Compared to these approaches, **MSDCRD** achieves effective knowledge transfer directly within the feature space using only a simple linear projector. On the CIFAR100 dataset, MSDCRD achieves state-of-the-art performance across nearly all heterogeneous model combinations. Notably, for ViT-based and MLP-based student networks, it delivers substantial gains over the second-best method,

with improvements ranging from 5.82% to 9.76%. However, when Mixer-B/16 is used as the teacher, the performance gains are relatively less significant compared to those achieved with other teacher-student pairs. A similar trend is observed on ImageNet, where MSDCRD outperforms existing methods in most settings. Yet, with Mixer-B/16 as the teacher, the improvements for both ResNet-18 and Swin-N students are relatively limited. We attribute this to the weaker baseline performance of Mixer-B/16 compared to other teacher models, which may hinder effective knowledge transfer. It is worth noting that our method achieves such competitive results using only single-layer features, whereas most other high-performing methods rely on multi-layer features, further demonstrating the efficiency and general applicability of our approach.

Table 10: **Results on object detection.** We use AP on different settings to evaluate results. “R101” denotes the use of ResNet-101 as backbone, and the same naming convention applies to other models.

Method		mAP	AP50	AP75	API	APm	APS
Teacher	Faster R-CNN w/ R101-FPN	42.04	62.48	45.88	54.60	45.55	25.22
Student	Faster R-CNN w/ R18-FPN	33.26	53.61	35.26	43.16	35.68	18.96
	w/ KD	33.97 (+0.61)	54.66	36.62	44.14	36.67	18.71
	w/ FitNet	34.13 (+0.87)	54.16	36.71	44.69	36.50	18.88
	w/ FIGI	35.44 (+2.18)	55.51	38.17	47.34	38.29	<b>19.04</b>
	w/ MSDCRD	<b>35.58</b> (+2.32)	<b>55.89</b>	<b>38.35</b>	<b>47.47</b>	<b>38.60</b>	18.45
Teacher	RetinaNet101	40.40	60.25	43.19	52.18	44.34	24.032
Student	RetinaNet50	36.15	56.03	38.73	46.95	40.25	21.37
	w/ KD	36.76 (+0.61)	56.60	39.40	48.17	40.56	21.87
	w/ FitNet	36.30 (+0.15)	55.95	38.95	47.14	40.32	20.10
	w/ FIGI	37.29 (+1.14)	57.13	40.04	<b>49.71</b>	41.47	21.01
	w/ MSDCRD	<b>37.67</b> (+1.52)	<b>57.63</b>	<b>40.39</b>	48.95	<b>41.65</b>	<b>22.15</b>

## C Object Detection

Since most knowledge distillation methods are primarily designed for classification tasks, only a few [11, 13] apply to object detection. In recent years, a number of distillation methods specifically designed for object detection tasks have been proposed. Among them, we select the FIGG [45] method as a representative and widely adopted baseline. FIGG is designed to address the inherent imbalance between foreground and background regions by explicitly separating them and applying distillation only to the regions of interest.

### C.1 Dataset

We conduct our object detection experiments on the COCO 2017 dataset [42], a large-scale benchmark widely used for evaluating object detection and segmentation. The dataset contains over 118,000 training images and 5,000 validation images, annotated with bounding boxes and instance segmentation masks for 80 object categories. Its challenging nature, characterized by dense object layouts, large intra-class variance, and scale diversity, makes it a standard benchmark for assessing the performance and generalization of detection models.

### C.2 Implementation Details

For model implementation and training, we adopt Detectron2 [43], a high-performance object detection library developed by Facebook AI Research (FAIR). Built on PyTorch, Detectron2 provides a modular and extensible platform for implementing state-of-the-art detection algorithms, including Faster R-CNN, RetinaNet, and Mask R-CNN. All object detection experiments in this work are conducted using four NVIDIA 3090 GPUs.

### C.3 Results and Analysis

The comparison results are presented in Table 6 and Table 10. As shown, traditional classification-based methods such as KD and FitNet offer limited improvements when directly applied to detection

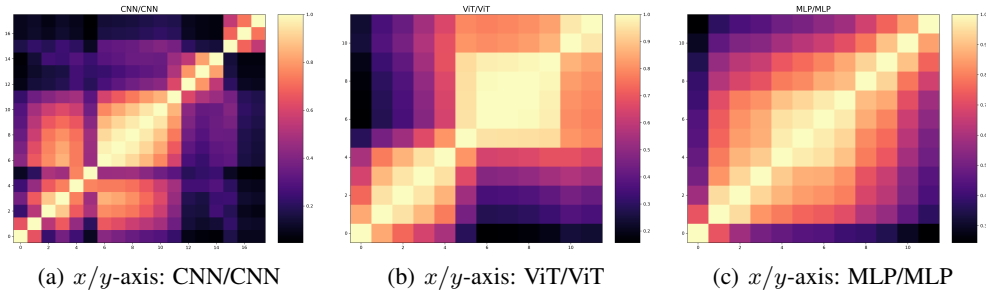


Figure 3: Similarity heatmap of intermediate features between homogeneous models measured by CKA. We compare features from ConvNeXt-T (CNN), ViT-Small (Transformer) and Mixer-B/16 (MLP model).

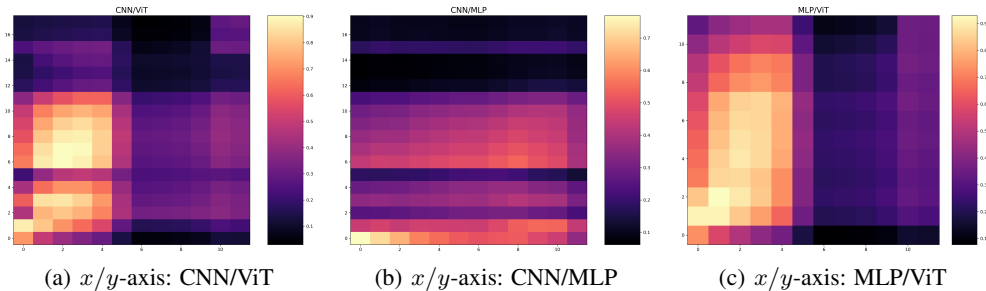


Figure 4: Similarity heatmap of intermediate features between Heterogeneous models measured by CKA. We compare features from ConvNeXt-T (CNN), ViT-Small (Transformer) and Mixer-B/16 (MLP model).

tasks. While FIFG achieves better performance due to its detection-aware design, our proposed method still consistently delivers superior results in all cases.

Moreover, we conduct experiments not only on two-stage detectors such as Faster R-CNN [46], but also on one-stage detectors like RetinaNet [47]. The results demonstrate that our approach significantly improves student model performance across different detection paradigms.

#### C.4 Extensibility of MSDCRD

Due to its plug-and-play nature and strong extensibility, MSDCRD holds great potential for integration with other advanced distillation techniques, offering further performance gains for student models.

### D Feature discrepancies between homogeneous and heterogeneous models.

To explicitly quantify the differences in feature representations across distinct model architectures, we adopt the Centered Kernel Alignment (CKA) [48, 49] as the similarity metric. Compared to other similarity measures such as cosine similarity, SVCCA, and PWCCA, CKA demonstrates superior stability and has been shown to perform more reliably in cross-architecture feature comparisons.

**Centered kernel alignment analysis.** CKA evaluates feature similarity over mini-batch. Given the output features of two different architectures on the same batch of input samples, denoted as  $X \in R^{n \times d_1}$ ,  $Y \in R^{n \times d_2}$ , where  $n$  is the number of samples in the batch and, without loss of generality, we assume that  $d_1 \neq d_2$ , the corresponding feature Gram matrices for  $X$  and  $Y$  are computed as follows

$$L = XX^T, K = YY^T \quad (13)$$

According to the Hilbert-Schmidt Independence Criterion (HSIC), its empirical estimation is given by

$$HSIC(K, L) = \frac{1}{(n-1)^2} tr(KHLH) \quad (14)$$

where  $H$  is the centering matrix  $H_n = I_n - \frac{1}{n}11^T$ .

HSIC is not inherently invariant to isotropic scaling; however, such invariance can be achieved by applying an appropriate normalization. The normalized version of HSIC is referred to as Centered Kernel Alignment (CKA)

$$CKA(K, L) = \frac{HSIC(K, L)}{\sqrt{HSIC(K, K)HSIC(L, L)}} \quad (15)$$

As illustrated in Figure 3 and Figure 4, we compute the CKA similarity between the output features of each block across different network architectures. Figure 3 presents the CKA heatmaps for networks with homogeneous architectures, where strong feature similarity is observed between blocks at the same position. In contrast, Figure 4 shows the CKA similarity between heterogeneous architectures, revealing a markedly different pattern: while some similarity may still exist in the early layers, deeper blocks, which typically capture higher-level semantic representations, exhibit little to no correlation. This observation highlights the intrinsic feature gap across heterogeneous models.

The inherent discrepancy in intermediate features across heterogeneous architectures primarily arises from differences in the architectures’ inductive biases. In CNNs, inductive biases such as locality, two-dimensional spatial structure, and translation equivariance are embedded throughout the whole network. In contrast, ViTs incorporate global self-attention layers that lack these biases, with only MLP sublayers exhibiting locality and translational equivariance. As a result, effective knowledge transfer across heterogeneous models remains a fundamental challenge in feature-based distillation.

## E Limitations

1. In this work, we focus solely on evaluating MSDCRD alone within classification and object detection tasks. Given its plug-and-play and flexible design, MSDCRD holds strong potential to be integrated with other distillation strategies across various vision tasks, offering a promising direction for exploring more efficient knowledge transfer.
2. This study concentrates on performing multi-scale decoupling within individual global features. However, in many feature distillation methods, features from multiple layers are often involved, and these inter-layer features exhibit inherent coupling. We encourage future work to investigate effective inter-layer decoupling strategies.

## NeurIPS Paper Checklist

The checklist is designed to encourage best practices for responsible machine learning research, addressing issues of reproducibility, transparency, research ethics, and societal impact. Do not remove the checklist: **The papers not including the checklist will be desk rejected.** The checklist should follow the references and follow the (optional) supplemental material. The checklist does NOT count towards the page limit.

Please read the checklist guidelines carefully for information on how to answer these questions. For each question in the checklist:

- You should answer [Yes], [No], or [NA].
- [NA] means either that the question is Not Applicable for that particular paper or the relevant information is Not Available.
- Please provide a short (1–2 sentence) justification right after your answer (even for NA).

**The checklist answers are an integral part of your paper submission.** They are visible to the reviewers, area chairs, senior area chairs, and ethics reviewers. You will be asked to also include it (after eventual revisions) with the final version of your paper, and its final version will be published with the paper.

The reviewers of your paper will be asked to use the checklist as one of the factors in their evaluation. While "[Yes]" is generally preferable to "[No]", it is perfectly acceptable to answer "[No]" provided a proper justification is given (e.g., "error bars are not reported because it would be too computationally expensive" or "we were unable to find the license for the dataset we used"). In general, answering "[No]" or "[NA]" is not grounds for rejection. While the questions are phrased in a binary way, we acknowledge that the true answer is often more nuanced, so please just use your best judgment and write a justification to elaborate. All supporting evidence can appear either in the main paper or the supplemental material, provided in appendix. If you answer [Yes] to a question, in the justification please point to the section(s) where related material for the question can be found.

IMPORTANT, please:

- **Delete this instruction block, but keep the section heading "NeurIPS Paper Checklist",**
- **Keep the checklist subsection headings, questions/answers and guidelines below.**
- **Do not modify the questions and only use the provided macros for your answers.**

### 1. Claims

Question: Do the main claims made in the abstract and introduction accurately reflect the paper's contributions and scope?

Answer: [Yes]

Justification: The main contributions and scope are summarized in the abstract and introduction.

Guidelines:

- The answer NA means that the abstract and introduction do not include the claims made in the paper.
- The abstract and/or introduction should clearly state the claims made, including the contributions made in the paper and important assumptions and limitations. A No or NA answer to this question will not be perceived well by the reviewers.
- The claims made should match theoretical and experimental results, and reflect how much the results can be expected to generalize to other settings.
- It is fine to include aspirational goals as motivation as long as it is clear that these goals are not attained by the paper.

### 2. Limitations

Question: Does the paper discuss the limitations of the work performed by the authors?

Answer: [Yes]

Justification: Limitations are discussed in Sec E in the Appendix.

Guidelines:

- The answer NA means that the paper has no limitation while the answer No means that the paper has limitations, but those are not discussed in the paper.
- The authors are encouraged to create a separate "Limitations" section in their paper.
- The paper should point out any strong assumptions and how robust the results are to violations of these assumptions (e.g., independence assumptions, noiseless settings, model well-specification, asymptotic approximations only holding locally). The authors should reflect on how these assumptions might be violated in practice and what the implications would be.
- The authors should reflect on the scope of the claims made, e.g., if the approach was only tested on a few datasets or with a few runs. In general, empirical results often depend on implicit assumptions, which should be articulated.
- The authors should reflect on the factors that influence the performance of the approach. For example, a facial recognition algorithm may perform poorly when image resolution is low or images are taken in low lighting. Or a speech-to-text system might not be used reliably to provide closed captions for online lectures because it fails to handle technical jargon.
- The authors should discuss the computational efficiency of the proposed algorithms and how they scale with dataset size.
- If applicable, the authors should discuss possible limitations of their approach to address problems of privacy and fairness.
- While the authors might fear that complete honesty about limitations might be used by reviewers as grounds for rejection, a worse outcome might be that reviewers discover limitations that aren't acknowledged in the paper. The authors should use their best judgment and recognize that individual actions in favor of transparency play an important role in developing norms that preserve the integrity of the community. Reviewers will be specifically instructed to not penalize honesty concerning limitations.

### 3. Theory assumptions and proofs

Question: For each theoretical result, does the paper provide the full set of assumptions and a complete (and correct) proof?

Answer: [Yes]

Justification: We have already provided the proof of theoretical results in the Methods section and the Appendix.

Guidelines:

- The answer NA means that the paper does not include theoretical results.
- All the theorems, formulas, and proofs in the paper should be numbered and cross-referenced.
- All assumptions should be clearly stated or referenced in the statement of any theorems.
- The proofs can either appear in the main paper or the supplemental material, but if they appear in the supplemental material, the authors are encouraged to provide a short proof sketch to provide intuition.
- Inversely, any informal proof provided in the core of the paper should be complemented by formal proofs provided in appendix or supplemental material.
- Theorems and Lemmas that the proof relies upon should be properly referenced.

### 4. Experimental result reproducibility

Question: Does the paper fully disclose all the information needed to reproduce the main experimental results of the paper to the extent that it affects the main claims and/or conclusions of the paper (regardless of whether the code and data are provided or not)?

Answer: [Yes]

Justification: We have already disclosed all the information needed to reproduce the main experimental results of the paper.

Guidelines:

- The answer NA means that the paper does not include experiments.
- If the paper includes experiments, a No answer to this question will not be perceived well by the reviewers: Making the paper reproducible is important, regardless of whether the code and data are provided or not.
- If the contribution is a dataset and/or model, the authors should describe the steps taken to make their results reproducible or verifiable.
- Depending on the contribution, reproducibility can be accomplished in various ways. For example, if the contribution is a novel architecture, describing the architecture fully might suffice, or if the contribution is a specific model and empirical evaluation, it may be necessary to either make it possible for others to replicate the model with the same dataset, or provide access to the model. In general, releasing code and data is often one good way to accomplish this, but reproducibility can also be provided via detailed instructions for how to replicate the results, access to a hosted model (e.g., in the case of a large language model), releasing of a model checkpoint, or other means that are appropriate to the research performed.
- While NeurIPS does not require releasing code, the conference does require all submissions to provide some reasonable avenue for reproducibility, which may depend on the nature of the contribution. For example
  - (a) If the contribution is primarily a new algorithm, the paper should make it clear how to reproduce that algorithm.
  - (b) If the contribution is primarily a new model architecture, the paper should describe the architecture clearly and fully.
  - (c) If the contribution is a new model (e.g., a large language model), then there should either be a way to access this model for reproducing the results or a way to reproduce the model (e.g., with an open-source dataset or instructions for how to construct the dataset).
  - (d) We recognize that reproducibility may be tricky in some cases, in which case authors are welcome to describe the particular way they provide for reproducibility. In the case of closed-source models, it may be that access to the model is limited in some way (e.g., to registered users), but it should be possible for other researchers to have some path to reproducing or verifying the results.

## 5. Open access to data and code

Question: Does the paper provide open access to the data and code, with sufficient instructions to faithfully reproduce the main experimental results, as described in supplemental material?

Answer: [NA]

Justification: The data and code will be released in camera ready.

Guidelines:

- The answer NA means that paper does not include experiments requiring code.
- Please see the NeurIPS code and data submission guidelines (<https://nips.cc/public/guides/CodeSubmissionPolicy>) for more details.
- While we encourage the release of code and data, we understand that this might not be possible, so “No” is an acceptable answer. Papers cannot be rejected simply for not including code, unless this is central to the contribution (e.g., for a new open-source benchmark).
- The instructions should contain the exact command and environment needed to run to reproduce the results. See the NeurIPS code and data submission guidelines (<https://nips.cc/public/guides/CodeSubmissionPolicy>) for more details.
- The authors should provide instructions on data access and preparation, including how to access the raw data, preprocessed data, intermediate data, and generated data, etc.
- The authors should provide scripts to reproduce all experimental results for the new proposed method and baselines. If only a subset of experiments are reproducible, they should state which ones are omitted from the script and why.
- At submission time, to preserve anonymity, the authors should release anonymized versions (if applicable).

- Providing as much information as possible in supplemental material (appended to the paper) is recommended, but including URLs to data and code is permitted.

## 6. Experimental setting/details

Question: Does the paper specify all the training and test details (e.g., data splits, hyper-parameters, how they were chosen, type of optimizer, etc.) necessary to understand the results?

Answer: [\[Yes\]](#)

Justification: The implementation details are thoroughly provided in both Sec B.1 and Sec C.2 of the Appendix, as well as in the Implementation Details section of the main manuscript.

Guidelines:

- The answer NA means that the paper does not include experiments.
- The experimental setting should be presented in the core of the paper to a level of detail that is necessary to appreciate the results and make sense of them.
- The full details can be provided either with the code, in appendix, or as supplemental material.

## 7. Experiment statistical significance

Question: Does the paper report error bars suitably and correctly defined or other appropriate information about the statistical significance of the experiments?

Answer: [\[No\]](#)

Justification: All reported results are averaged over experiments conducted with three different random seeds.

Guidelines:

- The answer NA means that the paper does not include experiments.
- The authors should answer "Yes" if the results are accompanied by error bars, confidence intervals, or statistical significance tests, at least for the experiments that support the main claims of the paper.
- The factors of variability that the error bars are capturing should be clearly stated (for example, train/test split, initialization, random drawing of some parameter, or overall run with given experimental conditions).
- The method for calculating the error bars should be explained (closed form formula, call to a library function, bootstrap, etc.)
- The assumptions made should be given (e.g., Normally distributed errors).
- It should be clear whether the error bar is the standard deviation or the standard error of the mean.
- It is OK to report 1-sigma error bars, but one should state it. The authors should preferably report a 2-sigma error bar than state that they have a 96% CI, if the hypothesis of Normality of errors is not verified.
- For asymmetric distributions, the authors should be careful not to show in tables or figures symmetric error bars that would yield results that are out of range (e.g. negative error rates).
- If error bars are reported in tables or plots, The authors should explain in the text how they were calculated and reference the corresponding figures or tables in the text.

## 8. Experiments compute resources

Question: For each experiment, does the paper provide sufficient information on the computer resources (type of compute workers, memory, time of execution) needed to reproduce the experiments?

Answer: [\[Yes\]](#)

Justification: All of our experiments were conducted on 3090 GPUs, with a maximum GPU memory of approximately 24 GB. For experiments on the CIFAR-100 dataset, we utilized a single 3090 GPU for both training and evaluation. For experiments on the ImageNet and COCO2017 datasets, we employed four 3090 GPUs.

Guidelines:

- The answer NA means that the paper does not include experiments.
- The paper should indicate the type of compute workers CPU or GPU, internal cluster, or cloud provider, including relevant memory and storage.
- The paper should provide the amount of compute required for each of the individual experimental runs as well as estimate the total compute.
- The paper should disclose whether the full research project required more compute than the experiments reported in the paper (e.g., preliminary or failed experiments that didn't make it into the paper).

#### 9. Code of ethics

Question: Does the research conducted in the paper conform, in every respect, with the NeurIPS Code of Ethics <https://neurips.cc/public/EthicsGuidelines>?

Answer: [Yes]

Justification: We conducted the research in the paper conform, in every respect, with the NeurIPS Code of Ethics.

Guidelines:

- The answer NA means that the authors have not reviewed the NeurIPS Code of Ethics.
- If the authors answer No, they should explain the special circumstances that require a deviation from the Code of Ethics.
- The authors should make sure to preserve anonymity (e.g., if there is a special consideration due to laws or regulations in their jurisdiction).

#### 10. Broader impacts

Question: Does the paper discuss both potential positive societal impacts and negative societal impacts of the work performed?

Answer: [NA]

Justification: There is no societal impact of the work performed.

Guidelines:

- The answer NA means that there is no societal impact of the work performed.
- If the authors answer NA or No, they should explain why their work has no societal impact or why the paper does not address societal impact.
- Examples of negative societal impacts include potential malicious or unintended uses (e.g., disinformation, generating fake profiles, surveillance), fairness considerations (e.g., deployment of technologies that could make decisions that unfairly impact specific groups), privacy considerations, and security considerations.
- The conference expects that many papers will be foundational research and not tied to particular applications, let alone deployments. However, if there is a direct path to any negative applications, the authors should point it out. For example, it is legitimate to point out that an improvement in the quality of generative models could be used to generate deepfakes for disinformation. On the other hand, it is not needed to point out that a generic algorithm for optimizing neural networks could enable people to train models that generate Deepfakes faster.
- The authors should consider possible harms that could arise when the technology is being used as intended and functioning correctly, harms that could arise when the technology is being used as intended but gives incorrect results, and harms following from (intentional or unintentional) misuse of the technology.
- If there are negative societal impacts, the authors could also discuss possible mitigation strategies (e.g., gated release of models, providing defenses in addition to attacks, mechanisms for monitoring misuse, mechanisms to monitor how a system learns from feedback over time, improving the efficiency and accessibility of ML).

#### 11. Safeguards

Question: Does the paper describe safeguards that have been put in place for responsible release of data or models that have a high risk for misuse (e.g., pretrained language models, image generators, or scraped datasets)?

Answer: [NA]

Justification: There are no such risks in this paper.

Guidelines:

- The answer NA means that the paper poses no such risks.
- Released models that have a high risk for misuse or dual-use should be released with necessary safeguards to allow for controlled use of the model, for example by requiring that users adhere to usage guidelines or restrictions to access the model or implementing safety filters.
- Datasets that have been scraped from the Internet could pose safety risks. The authors should describe how they avoided releasing unsafe images.
- We recognize that providing effective safeguards is challenging, and many papers do not require this, but we encourage authors to take this into account and make a best faith effort.

## 12. Licenses for existing assets

Question: Are the creators or original owners of assets (e.g., code, data, models), used in the paper, properly credited and are the license and terms of use explicitly mentioned and properly respected?

Answer: [Yes]

Justification: We strictly adhered to the MIT license terms for CIFAR-100, the Creative Commons Attribution 4.0 License (CC BY 4.0) terms for COCO 2017, and the ImageNet is available for non-commercial research purposes under a custom license.

Guidelines:

- The answer NA means that the paper does not use existing assets.
- The authors should cite the original paper that produced the code package or dataset.
- The authors should state which version of the asset is used and, if possible, include a URL.
- The name of the license (e.g., CC-BY 4.0) should be included for each asset.
- For scraped data from a particular source (e.g., website), the copyright and terms of service of that source should be provided.
- If assets are released, the license, copyright information, and terms of use in the package should be provided. For popular datasets, [paperswithcode.com/datasets](https://paperswithcode.com/datasets) has curated licenses for some datasets. Their licensing guide can help determine the license of a dataset.
- For existing datasets that are re-packaged, both the original license and the license of the derived asset (if it has changed) should be provided.
- If this information is not available online, the authors are encouraged to reach out to the asset's creators.

## 13. New assets

Question: Are new assets introduced in the paper well documented and is the documentation provided alongside the assets?

Answer: [NA]

Justification: The data and code will be released in camera ready.

Guidelines:

- The answer NA means that the paper does not release new assets.
- Researchers should communicate the details of the dataset/code/model as part of their submissions via structured templates. This includes details about training, license, limitations, etc.
- The paper should discuss whether and how consent was obtained from people whose asset is used.
- At submission time, remember to anonymize your assets (if applicable). You can either create an anonymized URL or include an anonymized zip file.

#### 14. Crowdsourcing and research with human subjects

Question: For crowdsourcing experiments and research with human subjects, does the paper include the full text of instructions given to participants and screenshots, if applicable, as well as details about compensation (if any)?

Answer: [NA]

Justification: This paper does not involve crowdsourcing nor research with human subjects.

Guidelines:

- The answer NA means that the paper does not involve crowdsourcing nor research with human subjects.
- Including this information in the supplemental material is fine, but if the main contribution of the paper involves human subjects, then as much detail as possible should be included in the main paper.
- According to the NeurIPS Code of Ethics, workers involved in data collection, curation, or other labor should be paid at least the minimum wage in the country of the data collector.

#### 15. Institutional review board (IRB) approvals or equivalent for research with human subjects

Question: Does the paper describe potential risks incurred by study participants, whether such risks were disclosed to the subjects, and whether Institutional Review Board (IRB) approvals (or an equivalent approval/review based on the requirements of your country or institution) were obtained?

Answer: [NA] .

Justification: This paper does not involve crowdsourcing nor research with human subjects.

Guidelines:

- The answer NA means that the paper does not involve crowdsourcing nor research with human subjects.
- Depending on the country in which research is conducted, IRB approval (or equivalent) may be required for any human subjects research. If you obtained IRB approval, you should clearly state this in the paper.
- We recognize that the procedures for this may vary significantly between institutions and locations, and we expect authors to adhere to the NeurIPS Code of Ethics and the guidelines for their institution.
- For initial submissions, do not include any information that would break anonymity (if applicable), such as the institution conducting the review.

#### 16. Declaration of LLM usage

Question: Does the paper describe the usage of LLMs if it is an important, original, or non-standard component of the core methods in this research? Note that if the LLM is used only for writing, editing, or formatting purposes and does not impact the core methodology, scientific rigor, or originality of the research, declaration is not required.

Answer: [NA]

Justification: The core method development in this research does not involve LLMs as any important, original, or non-standard components.

Guidelines:

- The answer NA means that the core method development in this research does not involve LLMs as any important, original, or non-standard components.
- Please refer to our LLM policy (<https://neurips.cc/Conferences/2025/LLM>) for what should or should not be described.